Research Paper

Improving the Efficacy of Photoimmunotherapy (PIT) using a Cocktail of Antibody Conjugates in a Multiple Antigen Tumor Model

Takahito Nakajima, Kohei Sano, Peter L. Choyke, and Hisataka Kobayashi ✉

Molecular Imaging Program, Center for Cancer Research, National Cancer Institute, National Institutes of Health, Bethesda Maryland 20892, United States

✉ Corresponding author: Hisataka Kobayashi, M.D., Ph.D. Molecular Imaging Program, Center for Cancer Research, National Cancer Institute, NIH, Building 10, RoomB3B69, MSC1088, Bethesda, MD 20892-1088. Phone: 301-451-4220, Fax: 301-402-3191. E-mail: Kobayash@mail.nih.gov

Abstract

Tumors are characterized by a high degree of diversity and heterogeneity in receptor expression. Monoclonal antibodies (mAbs) are an established therapeutic method of targeting cell surface receptors. However, high affinity antibodies targeting highly expressed receptors are often prevented from distributing evenly throughout the tumor due to the "binding site barrier" whereby antibody is trapped peripherally before it can reach deeper into the tumor that leads inhomogeneous micro-distribution. When employing armed antibodies it is important that the toxin (in this case, phototoxin) be distributed evenly to more effectively treat the cancer. By adding an additional antibody conjugate, targeting a secondary, unsaturated receptor with lower expression, a more uniform distribution of the phototoxin can be achieved. In this study, panitumumab (Pan) and basiliximab (Bas) were conjugated with the phthalocyanine dye, IRDye700DX (IR700). Upon exposure to near infrared light, these armed antibodies produce rapid cell death only when bound to their respective receptors, a treatment termed photo-immunotherapy (PIT). ATAC4 cells which demonstrate high expression of human epidermal growth factor receptor (EGFR) and low expression of interleukin-2 receptor-alpha (CD25) were treated by PIT using a cocktail of Pan-IR700 and Bas-IR700. *An in vivo* study showed that the cocktail Pan-Bas-IR700 resulted in significantly reduced tumor growth and prolonged survival in ATAC4 tumor-bearing mice compared with either Pan-IR700 or Bas-IR700 alone. In conclusion, a cocktail injection of two different antibody-IR700 conjugates created a more homogeneous microdistribution of antibody-conjugates resulting in enhanced therapeutic effects after PIT, compared to the use of either antibody-IR700 conjugate.

Key words: photoimmunotherapy; monoclonal antibody; cocktail; micro-distribution; binding site barrier

Introduction

Growing numbers of intact and armed monoclonal antibodies (mAbs) have been used for targeted cancer therapy and demonstrate effective tumor control usually when combined with conventional therapies (1–4). MAbs with high affinity are generally preferable in pharmacokinetics for targeting cancers in vivo because of their stable binding to target molecules that leads to high tumor to background ratios

(TBR). However, one recognized limitation of mAb-based therapy is the inhomogeneous intra-tumoral distribution of antibodies (5–7). This occurs especially when a mAb has a high binding affinity for its receptor and/or the tumor cells express high levels of target antigen. In this case mAbs are saturated in the immediate perivascular space and cannot penetrate deeper into the tumor, a phenomenon known as the "binding site barrier" (8–14). More uniform distribution of antibodies can be achieved by adding a second mAb with either lower affinity or lower antigen expression which enables this second mAb to be more bioavailable deeper in the tumor.

Photoimmunotherapy (PIT) is a newly described form of mAb-conjugate image-guided therapy, in which a phthalocyanine dye, IRDye700DX (IR700), is conjugated to the mAb. Subsequently, near infrared (NIR) light exposure leads to nearly immediate, target-selective necrotic cell death both *in vitro* and *in vivo* (15). Therefore, a desirable requisite for PIT is homogeneous distribution of antibody conjugates, to enable uniform distribution of the IR700 dye throughout the tumor. A cocktail containing a high affinity primary mAb-IR700 conjugate targeting high expression antigens combined with a secondary mAb-IR700 conjugate targeting moderately expressed antigens, would be anticipated to lead to a more homogeneous distribution of IR700 throughout the tumor, than either mAb-IR700 conjugate alone. We therefore propose that a "cocktail" of two mAbs against two distinct targeting antigens with higher and lower expression, respectively on the surface of target cancer cells, should improve the homogeneity of mAb-binding to cancer cells *in vivo*, resulting in superior PIT effectiveness in tumor control.

In this study, a cocktail of two different mAbs-IR700 conjugates, a primary mAb against human epidermal growth factor receptor (EGFR) and a secondary mAb against interleukin-2 receptor-alpha (CD25, Tac antigen), both conjugated with IR700, was employed in mice with implanted ATAC4 tumors to investigate the advantages of using a cocktail of two mAb-IR700 conjugates with PIT compared to either conjugate alone.

Materials and Methods

Reagents

A water-soluble, silica−phthalocyanine derivative, IRDye 700DX NHS ester (IR700; $C_{74}H_{96}N_{12}Na_4O_{27}S_6Si_3$, molecular weight 1954.22), was obtained from LI-COR Bioscience. Panitumumab, a fully humanized IgG2 mAb directed against the HER1 (EGFR), was purchased from Amgen. Basiliximab, a chimeric (murine/human) IgG1k mAb, specifically binding to CD25 was purchased from Novartis. The NHS esters of Alexa Fluor488 (Alexa488) and Texas Red-X (TexRed) were purchased from Invitrogen Corporation. All other chemicals used were of reagent grade.

Synthesis of IR700-conjugated antibodies

Panitumumab (1mg, 6.8nmol) was incubated with IR700 (60.2μg, 30.8nmol, 5mmol/L in DMSO) in 0.1 mol/L Na_2HPO_4 (pH 8.5) at room temperature for 1 h. The mixture (Pan-IR700) was purified with a Sephadex G50 column (PD-10; GE Healthcare). Basiliximab (1mg, 6.9nmol) was incubated with IR700 (61.1μg, 31.3 nmol, 5 mmol/L in DMSO) in the same manner Pan-IR700. Panitumumab and Basiliximab were incubated with NHS esters of TexRed and Alexa488 (70nmol) in the same manner as above, respectively (Pan-TexRed, Bas-Alx488). The protein concentration was determined with a Coomassie Plus protein assay kit (Thermo Fisher Scientific Inc.) by measuring the absorption at 595 nm with spectroscopy (8453 Value System; Agilent Technologies). The concentration of IR700 was measured by absorption with spectroscopy and the number of fluorophore molecules per basiliximab or panitumumab was adjusted to approximately 4.

Cell line

The ATAC4 cell line was generated by genetically transfecting the plasmid encoding CD25 and a neomycin-resistant gene into EGFR-expressing A43l cells (16,17). ATAC4 were grown in RPMI 1640 supplemented with 10% fetal bovine serum and 1% penicillin/streptomycin in tissue culture flasks in a humidified incubator at 37 °C in an atmosphere of 95% air and 5% carbon dioxide.

Fluorescence microscopy

ATAC4 cells (1×10^4) were plated on a covered glass-bottomed culture well and incubated for 16 hours. Pan-IR700, Bas-IR700 or both (Pan-Bas-IR700) (10μg/mL) were then added to ATAC4 cells, respectively. The cells were incubated for either one or six hours followed by washing once with PBS. Fluorescence microscopy was performed using an Olympus BX61 microscope (Olympus America, Inc.) equipped with the following filters: excitation wavelength 590 to 650 nm, emission wavelength 665 to 740 nm for IR700. Transmitted light differential interference contrast (DIC) images were also acquired.

Flow cytometry studies

For each measurement, data from 10,000 events were collected with a FACS Calibur flow cytometer

(BD Biosciences) and Cell Quest software (BD Biosciences), equipped with an argon-ion laser (488 nm) and diode laser (635 nm). Signals from cells were collected using FL1 emission filter (530/30nm, BP) for Bas-Alx488, FL2 (585/42 nm, BP) for PI and FL4 (661/16, BP) for IR700-conjugated mAb.

One-color flow cytometry was performed to evaluate the consistency of cell surface receptor density in ATAC4 cells. ATAC4 cells (3×10^4) were plated on a 24-chamber culture well and incubated for 16 h and the cells were incubated with Pan-IR700, Bas-IR700 or both at 37.0 °C for 6 h. Cells were then washed once with PBS, trypsinized, and flow cytometry was performed. Relative CD25 sites per cell were calculated by multiplying the geometric mean by the constant number, which was determined using known EGFR numbers per cell (1.5×10^6) divided by the geometric mean of cell numbers binding Pan-IR700.

To validate the specific binding of the antibody, excess antibody, panitumumab or basiliximab (500µg), were used to block 5µg of Pan-IR700, Bas-IR700 or a combination of both conjugates, respectively.

To further validate the expression of both EGFR and CD25, *in vivo*, two-color flow cytometry was performed with *ex vivo* tissue samples. ATAC4 tumor-bearing mice were euthanized with carbon oxide and ATAC4 tumors were harvested. Samples were cut into fragments of less than 1 mm³ and mechanically separated in PBS. Suspensions were then passed over a nylon sieve with a 70 µm pore size (Cell strainer; BD Biosciences) and were collected into 50 mL aliquots diluted in PBS. These cells were divided into 4 centrifuge tubes and were incubated with Pan-IR700, Bas-alx488 or both Pan-IR700 and Bas-Alx488, or without any conjugates as a control at 37 °C for 3h. Dead cells were stained with propidium iodine (PI) and were gated by flow cytometry.

Photoimmunotherapy *in vitro*

ATAC4 cells were seeded into 35 mm cell-culture dishes and incubated at 37 °C. After 24 h incubation, Bas-IR700 alone, Pan-IR700 alone or both were administrated at 10µg/ml. As a control, ATAC4 seeded dishes were prepared without the addition of any agents. Then, these dishes were incubated for 6 h at 37 °C. Cells followed by irradiation with light from an LED light source (L690−66−60, Marubeni America Co.) at wavelengths of 670–710 nm (peak at 690 nm) and a power density of 50mW/cm², as measured with an optical power meter (PM 100, Thorlabs). The doses of LED-irradiation for each dish were 0, 0.1, 0.2, 1 and 2 J/cm², respectively. Additionally, the irradiation at

the doses of 5 and 10 J/cm² was performed for control cells and ATAC4 cells incubated with Bas-IR700. After irradiation, dishes were washed with phosphate buffered saline (PBS) and cells were harvested and resuspended with PBS containing 2µg of PI per milliliter. The samples were then analyzed by flow cytometry.

Tumor model

All *in vivo* procedures were conducted in compliance with the Guide for the Care and Use of Laboratory Animal Resources (1996), U.S. National Research Council, and approved by the local Animal Care and Use Committee. Six- to eight-week-old female homozygous athymic nude mice were purchased from Charles River (NCI-Frederick). Two million ATAC4 cells were injected subcutaneously in the right dorsum of the mice. Tumor dimensions (length and width) were determined by caliper measurements. The volume was calculated by the following formula; tumor volume = length × width 1 × width 2 × 0.5. Tumors reaching approximately 40 mm³ in volume were selected for study.

In Vivo photoimmunotherapy in ATAC4 tumors with IR700-conjugated antibody

Selected mice were randomized into 7 groups of at least 10 animals per group for the following treatments: (1) no treatment (control); (2) 100µg of Pan-IR700 i.v., NIR light was administered at 50 J/cm² on day 1 after injection and 100 J/cm² on day 2 after injection (Pan-1PIT); (3) 100µg of Bas-IR700 i.v., NIR light was administered at 50 J/cm² on day 1 after injection and 100 J/cm² on day 2 after injection (Bas-1PIT); (4) both 100µg of Bas-IR700 and 100µg of Pan-IR700, NIR light was administered at 50 J/cm² on day 1 after injection and 100 J/cm² on day 2 after injection (Pan-Bas-1PIT); (5) 100µg of Pan-IR700 i.v. every four days for 12 days, NIR light was administered at 50 J/cm² one day after completion of the injection and 100 J/cm² on day 2 after injection (Pan-3PIT); (6) 100µg of Bas-IR700 i.v. every four days for 12 days, NIR light was administered at 50 J/cm² one day after completion of the injection and 100 J/cm² on day 2 after injection (Bas-3PIT); (7) both 100 µg of Bas-IR700 and 100µg of Pan-IR700 i.v. every four days for 12 days, NIR light was administered at 50 J/cm² on day 1 after completion of the injection and 100 J/cm² on day 2 after injection (Pan-Bas-3PIT).

Mice were monitored daily, and tumor volumes were measured two or three times a week. An LED light source was used for NIR irradiation of PIT at a power density of 200mW/cm². Fluorescence images, as well as white light images, were obtained using a

Pearl Imager (LI-COR Biosciences) with a 700 nm fluorescence channel with a 685 nm laser excitation.

Histological analysis

To investigate the microdistribution of each mAb in ATAC4 tumors, both Pan-TexRed and Bas-Alex488 were employed and were intravenously administrated into ATAC4 tumor bearing mice at a dose of 100µg each. Mice were euthanized with carbon dioxide 24 h after administration of the fluorescently labeled antibodies. ATAC4 tumors were harvested and were snap-frozen in OCT compound and then stored at −70 °C. Microscopic fluorescence images of the frozen sections of tissue samples were acquired as 10µm slice sections on slide glasses without staining. To detect TexRed and Alexa488 fluorescence a filter set of a 590−650 nm excitation filter and a 665−740 nm band-pass emission filter was employed.

Statistical analysis

Data are expressed as mean ± s.e.m. Statistical analyses were carried out using a statistics program (GraphPad Prism; GraphPad Software Inc.). The one-way analysis of variance (ANOVA) with post-test (Kruskal–Wallis test with post-test) was used to compare the tumor sizes to the other groups. The cumulative probability of survival (based on the failure of the tumor to reach 800 mm^3) was estimated in each group with the use of the Kaplan−Meier survival curve analysis, and the results were compared with use of the log-rank test.

Results

A comparison of EGFR and CD25 expression in ATAC4

Pan-IR700, Bas-IR700 and Pan-Bas-IR700 demonstrated intense fluorescence signal in ATAC4 cells. Blocking experiments using 100-fold excess levels of unlabeled Pan or Bas showed almost competitive blocking of their respective mAb-IR700 conjugates (Fig.1A); Uptakes of Pan-IR700 or Bas-IR700 were blocked independently by administration of either excess Pan or Bas (Fig. 1B). These blocking experiments validated that each mAb demonstrated specific binding for each antigen on the cell surface.

Since the ratios of dye to protein between Pan-IR700 and Bas-IR700 were almost the same, (approximately 4:1), the number of CD25 on ATAC4 cell surface was estimated from EGFR-derived fluorescence signal intensity and known EGFR expression on A431, (1.5 x 10^6), and the relative fluorescence signal of ATAC4 cells incubated with Pan-IR700. The number of CD25 receptors was estimated at 0.3 × 10^6 and total number of receptors including EGFR and CD25 was estimated to be 1.7 × 10^6. These values are consistent with prior reports (17,18).
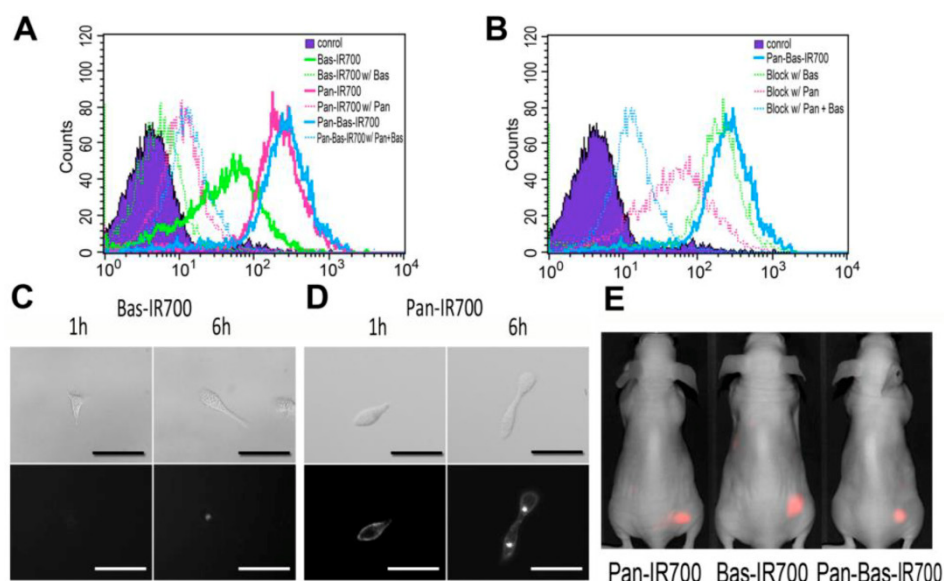

Figure 1. Histograms for flow cytometry of ATAC4 cells 6 hours after incubation with mAb linked to IR700. A, Blocking experiments using unlabeled mAb. Solid lines show histograms of ATAC4 cells binding with mAb-IR700 and dotted lines show the effect of blocking with unlabeled mAb. B, Blocking experiments with Pan-IR700 and Bas-IR700. Dotted lines showed histograms of ATAC4 cells with independent mAb employed as blocking agents. Serial DIC (upper row) and fluorescence microscopy (lower row) studies. Scale bars, 50µm. C, ATAC4 cells were incubated at 10µg/mL of Bas-IR700 for 1 or 6 hours. The fluorescence signal on the cell surface is barely visible at 1 or 6h incubation. For 6h incubation, focal accumulation of IR700 conjugates appeared inside the cell. D, ATAC4 cells were incubated with 10µg/mL of Pan-IR700 for 1 or 6 hours. The fluorescence signals were distributed uniformly on the cell surface after 1h or 6h incubation. Intracellular foci were seen after 6h. E, In vivo images of ATAC4 tumor-bearing mice 24h after administration of IR700-conjugates were acquired using a Pearl imager. No significant difference was seen in the appearance of the images.

To investigate the expression of targeted antigens on ATAC4 cells, *in vitro* fluorescence microscopy studies were performed after 1 and 6 h incubation with Pan-IR700 and Bas-IR700. At one hour, Pan-IR700 showed much greater fluorescence than Bas-IR700. At 6 hours, fluorescent dots were detected within the cytoplasm with both conjugates, but a much weaker signal was detected with Bas-IR700 (Fig. 1CD).

These experiments demonstrated that EGFR expression was much greater than CD25 expression on ATAC4 cells.

PIT with Bas-IR700 produces less cell death than Pan IR700 in ATAC4 cells *in vitro*

After Pan IR700 or Pan-Bas IR700 administration, NIR exposure at a dose of 2.0 J/cm^2 eradicated almost 100% of ATAC4 cells. There was no significant difference in the cell killing between Pan IR700 and Pan-Bas-IR700. The effect of PIT using Bas-IR700 was very much reduced compared to Pan-R700. Additionally, ATAC4 cells that did not receive either Pan-IR700 or Bas-IR700 were not affected by light irradiation even at high light doses up to 10 J/cm^2 (Fig. 2).
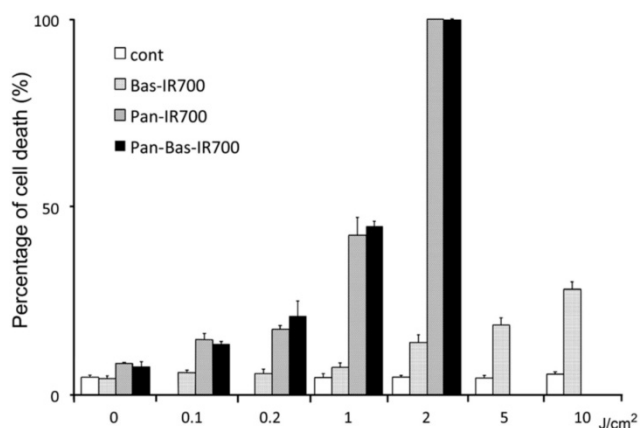

Figure 2. Cell death under various PIT conditions. Flow cytometry was performed after treatment to identify dead cells. Living ATAC4 cells were treated by PIT 24h after incubation with mAb-IR700 conjugates. Control cells were just exposed to NIR light.

In vivo microdistribution of Pan-TexRed and Bas-Alx488

To investigate the distribution of Pan and Bas in tumor tissue *in vivo*, Pan-TexRed and Bas-Alx488 were injected intravenously. Microscopic fluorescence images of the frozen sections of tissue samples were acquired 24 h after injection. Both conjugates were seen in the superficial areas of the tumor. Pan-TexRed was

mostly detected in the tumor periphery consistent with a binding site barrier due to the high expression of EGFR on ATAC4 cells and the high affinity of Pan to EGFR. In contrast, Bas-Alx488 distributed more homogenously throughout the tumor including in deeper regions (Fig. 3A).

Thus, when simultaneously showing distributions of both antibodies, Pan-TexRed was seen peripherally and Bas-Alx488 localized more centrally within the tumor (Fig. 3B). The tumor expression levels were relatively uniform throughout as the tumor was monoclonal and two-color flow cytometry confirmed that both antigens were present on ATAC4 cells from various sites within the tumor nodules.

Live ATAC4 cells were gated by manual regions of interest based on FL2 signals to omit dead cells by dead/live staining using PI. Flow cytometry allowed four dominant populations to be visualized: (1) FL1 (Alexa488) and FL4 (IR700)-negative dominant population in control cells; (2) FL1-negative and FL4-positive dominant population in cells incubated with Pan-IR700; (3) FL1-positive and FL4-negative dominant population in cells incubated with Bas-Alx488; (4) FL1 and FL4-positive population in cells with the cocktail of Pan-IR700 and Bas-Alx488. This confirms antigen expression was maintained throughout the ATAC4 tumor and differences in antibody distribution were therefore due to high affinity barrier effects (Fig. 3C).

Tumor response to PIT with a cocktail of Pan-IR700 and Bas-IR700

The efficacy of PIT was studied in 9 groups of ATAC4 tumor bearing mice (n = 10 mice in each group). After 100μg of Pan−IR700 i.v. injection on the day prior to PIT, ATAC4 tumors were treated with NIR light on day 1 (50 J/cm^2), day 2 (100 J/cm^2) except for three groups without NIR irradiation.

Repeated NIR irradiation (repeated PIT) demonstrated marked reduction in the size of ATAC4 tumors for each single mAb-IR700 or combined (Pan-Bas-IR700) administration of agents (19). Tumor volume was significantly reduced in ATAC4 tumors exposed to 3 treatments with PIT after, Bas-IR700, Pan-IR700 or both, compared with untreated control mice at day 10 (P < 0.0001). At day22 or later, Pan-Bas-3PIT had significant tumor size reductions compared with Bas-3PIT or Pan-3PIT. Single PIT also had significant reductions of tumor sizes compared with control mice at day10 except Bas-1PIT (Bas-1PIT; n.s, Pan-1PIT; P < 0.01, Pan-Bas-1PIT; P < 0.001) (Fig. 4 AB).

Survival analysis revealed that PIT repeated 3 times, resulted in prolonged survival with Bas-IR700,

Pan-IR700 or both (P < 0.001) (Fig. 4 CD). Pan-1PIT and Pan_Bas-1PIT had significant impact on mice

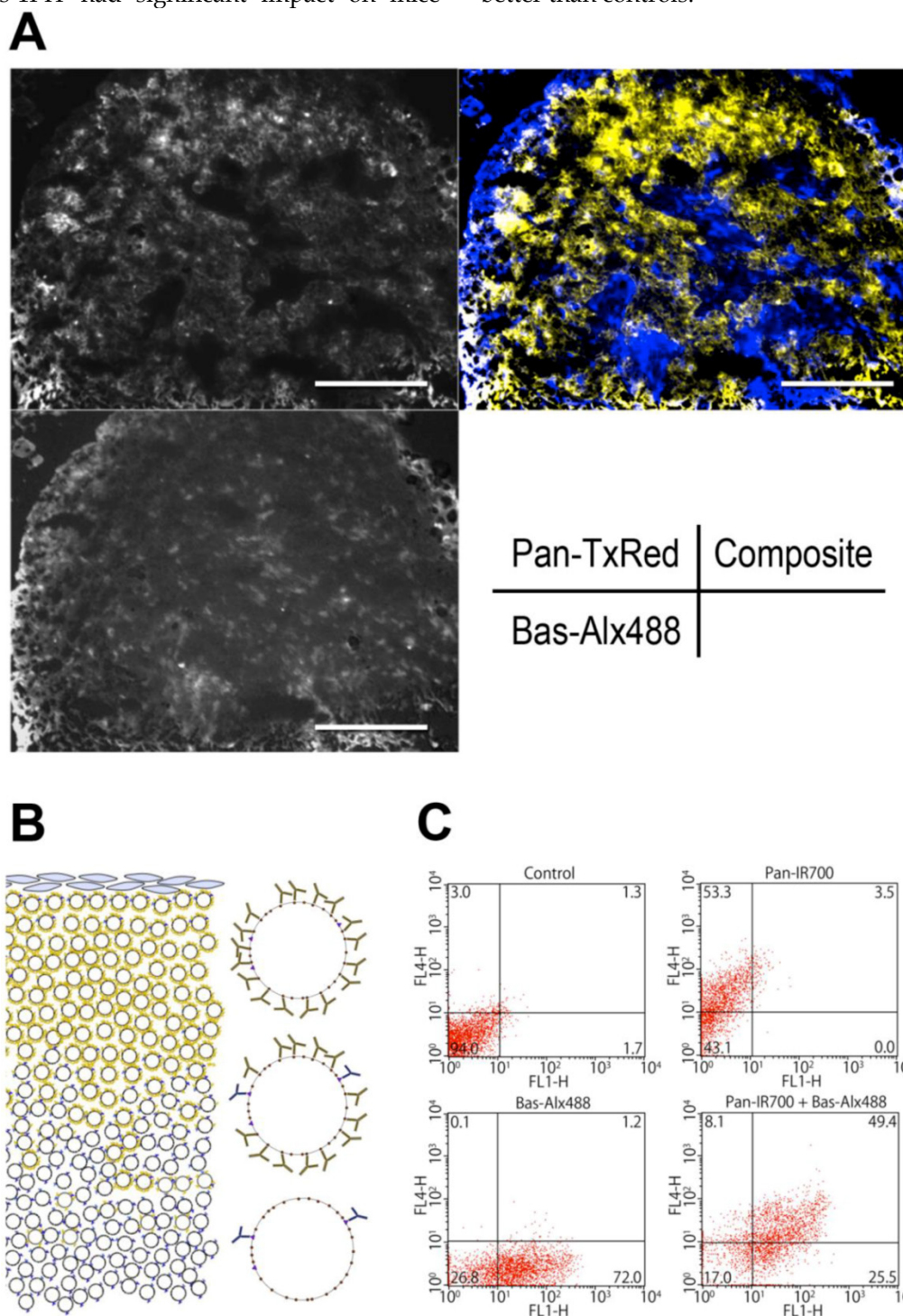survival (P < 0.05), but Bas-1PIT was not significantly better than controls.

Figure 3. A, Microdistribution of Bas and Pan in ATAC4 tumors. Pan-TexRed and Bas-Alx488 was administrated into ATAC4 tumor bearing mice 24 h before tumor tissues were excised from mice. Fluorescence microscopy of frozen sections of excised tumors was performed. Pan-TexRed was distributed in the superficial regions of the tumor, while Bas-Alx488 was found more homogenously Therefore, the composite image showed Pan-TexRed distributed peripherally, while Bas-Alx488 was found more centrally. B, A schematic for explaining the distribution of mAbs within a tumor. In the case of ATAC4 cells, excess EGFR antigen traps Pan-IR700 in the peripheral regions of the tumor especially around vessels preventing Pan-IR700 from penetrating more deeply in the tumor. Since Bas-IR700 has less antigen expression on ATAC4 cells (EGFR >> CD25), there is no barrier to its deeper penetration. This results in a more uniform distribution of IR700 throughout the tumor. C, Two-color flow cytometry of ex vivo ATAC4 cells. Pan-IR700 and Bas-Alx488 were incubated with.ATAC4 cells which were subjected to two-color flow cytometry to evaluate the expression of the antigens, EGFR and CD25. Most ATAC4 cells expressed both antigens throughout the tumor.
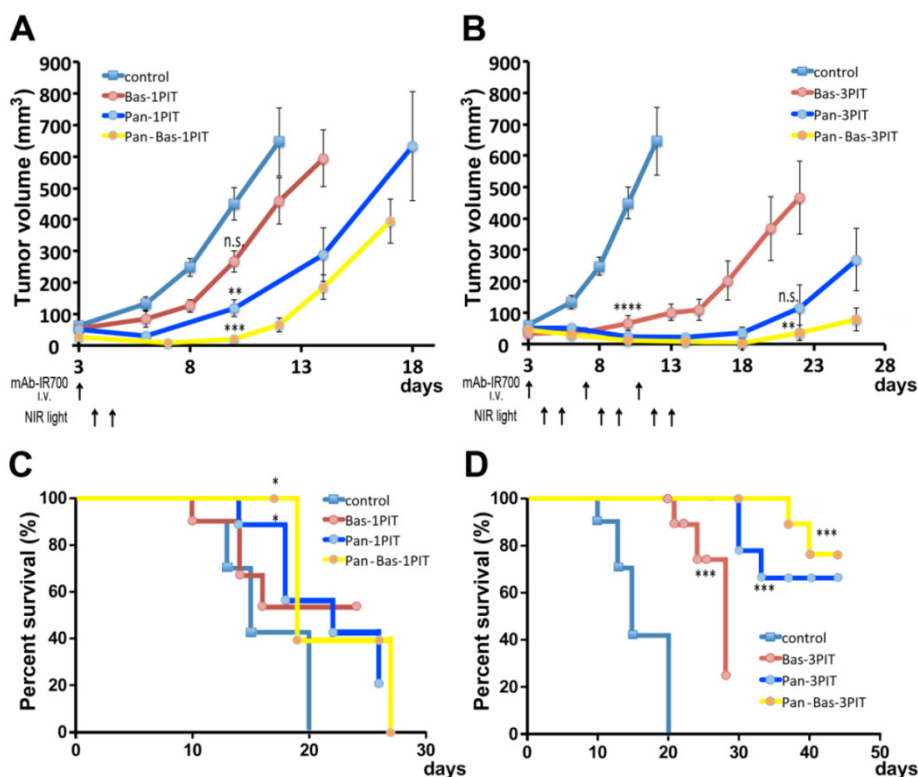
Figure 4. Tumor volume reduction in response to single PIT (A, C) and triple repeated PIT (B, D). Comparison in tumor sizes for each group at day 10 resulted in significant differences between the groups except Bas-1PIT. On day22 for 3PIT groups, Pan-Bas-3PIT had significant reductions of tumor sizes compared with Bas-3PIT, but Pan-3PIT had no significant difference with Bas-3PIT. PIT led to prolonged survival for all groups compared to control mice, except for Bas-1PIT. (* P <0.05, ** P < 0.01, *** P < 0.001, **** P < 0.0001)

Discussion

The results of PIT between *in vitro* and in vivo had clear discrepancy. In *in vitro* studies, cytotoxic effects of PIT with Pan-IR700 or Pan-Bas-IR700 showed no difference as expected. However, PIT with Pan-Bas-IR700 had a significant advantage *in vivo* over PIT with Pan-IR700 or Bas-IR700.

EGFR expression is approximately 6-fold greater than that of CD25 on ATAC4 cells (16, 17, 20–23). Therefore, *in vitro* PIT with 2.0J/cm² of NIR irradiation after administration of Pan-IR700 or Pan-Bas-IR700 resulted in 100 percent killing of exposed ATAC4 cells because virtually all cells expressed EGFR and Pan has high affinity with no barrier for binding *in vitro*. The effect of adding Bas-IR700 was minimal *in vitro*. The same amount of NIR irradiation after administration of Bas-IR700 killed only 15 percent of cells. In contrast to the *in vitro* studies, *in vivo* studies demonstrated that the best results were achieved using a cocktail of Pan-IR700 and Bas-IR700 because binding site barriers were overcome and resulted in a more homogeneous distribution of IR700 throughout the tumor. Therefore, the effect of adding

Bas-IR700 was much more significant *in vivo* than *in vitro* (8–14,24).

As shown in the microdistribution study, although receptor expression is uniform across the tumor, the Pan-IR700 was found more peripherally, whereas the Bas-IR700 distributed throughout the tumor but notably within the tumor's center, where Pan-IR700 was not found. Thus, PIT, with a cocktail Pan-Bas-IR700, was more effective than PIT with either mAb conjugate alone. PIT obtained after the antibody cocktail demonstrated more initial tumor shrinkage and prolonged survival compared with both controls because of the more homogeneous microdistribution of IR700 when using the cocktail. Fazio and Paganelli briefly addressed a cocktail usage of 2 different radiolabeled antibodies for radioimmunodetection and radioimmunotherapy to overcome "binding site barrier" (25). Our study is the first experimental demonstration of this hypothesis.

A potential alternative would be the use of fluorescent proteins (FPs), which are excellent endogenous fluorescence emitters or singlet oxygen producers to be used for depicting various biological processes or killing FP-expressing cells, respectively, both *in vitro* and *in vivo*. A recently reported alternative

technology to this target-specific PIT method is the tumor-specific imaging and therapy using telomerase promoter-regulated expression of various fluorescent proteins, which are induced with the adenovirus-mediated gene transfection *in vivo* (26–29). However, for the medical application, fluorescence proteins require virus-mediated *in vivo* gene transfection, which is unlikely to be permitted in humans at least in the near term. In contrast, this PIT technology can be used with injection of antibody-IR700 conjugates followed by NIR light exposure that could easily clear the current regulatory process.

Our data demonstrate that PIT is more effective when there is repeated NIR exposure, even without additional injection of mAb-IR700 conjugates (19). This is likely because after the first PIT, circulating mAb-IR700 can more freely leak into the tumor space leading to further binding of the mAb-IR700 within the tumor. Therefore, a repeat exposure to NIR light provides better access to cells that did not bind to mAb on the initial PIT. The repeat exposure to NIR light showed superior therapeutic effects including growth delay of tumor and prolonged survival of tumor bearing mice.

This study demonstrates that a cocktail injection of two different mAb-IR700 conjugates in tumors containing cells with differential expression of two or more antigens, results in a more homogeneous distribution of mAb conjugate across the tumor in vivo. This, in turn, results in better response to PIT because of the more even distribution of the phototoxin, IR700.

In conclusion, in ATAC4 tumors differentially expressing EGFR and CD25, *in vivo* PIT with a cocktail administration of Pan-IR700 and Bas-IR700 showed better efficacy than either antibody alone. *In vitro* results were misleading in this respect since *in vitro* cytotoxicity of PIT was simply depending on antibody-IR700 numbers bound to cells, therefore, they demonstrated complete cell killing with only the more highly expressed mAb-receptor pair. It is possible that even more complex combinations of mAb-IR700 conjugates, which have different affinity or different copies of targeting antigen expression, could be deployed in appropriate tumors to effectively cover the entire population of cancer cells within a tumor including treatment resistant cancer stem-like cells, yielding superior responses.

Acknowledgements

Competing Interests

The authors have declared that no competing interest exists.

References

1. Waldmann TA. Immunotherapy: past, present and future. Nat Med. 2003; 9:269-77.
2. Reichert JM, Rosensweig CJ, Faden LB, Dewitz MC. Monoclonal antibody successes in the clinic. Nat Biotechnol. 2005; 23:1073-8.
3. Pastan I, Hassan R, Fitzgerald DJ, Kreitman RJ. Immunotoxin therapy of cancer. Na Nat Rev Cancer. 2006; 6:559-65.
4. Goldenberg DM, Sharkey RM, Paganelli G, Barbet J, Chatal J-F. Antibody pretargeting advances cancer radioimmunodetection and radioimmunotherapy. J Clin Oncol. 2006; 24:823-34.
5. Jain RK, Baxter LT. Mechanisms of heterogeneous distribution of monoclonal antibodies and other macromolecules in tumors: significance of elevated interstitial pressure. Cancer Res. 1988; 48:7022-32.
6. Graff CP, Wittrup KD. Theoretical analysis of antibody targeting of tumor spheroids: importance of dosage for penetration, and affinity for retention. Cancer Res. 2003;63: 1288-96.
7. Thurber GM, Schmidt MM, Wittrup KD. Antibody tumor penetration: transport opposed by systemic and antigen-mediated clearance. Adv Drug Deliv Rev. 2008; 60:1421-34.
8. Fujimori K, Covell DG, Fletcher JE, Weinstein JN. Modeling analysis of the global and microscopic distribution of immunoglobulin G, F(ab')2, and Fab in tumors. Cancer Res. 1989; 49:5656-63.
9. Fujimori K, Covell DG, Fletcher JE, Weinstein JN. A modeling analysis of monoclonal antibody percolation through tumors: a binding-site barrier. J Nucl Med. 1990; 31:1191-8.
10. van Osdol W, Fujimori K, Weinstein JN. An analysis of monoclonal antibody distribution in microscopic tumor nodules: consequences of a "binding site barrier". Cancer Res. 1991; 51:4776-84.
11. Juweid M, Neumann R, Paik C, Perez-bacete MJ, Sato J, Osdol WV, et al. Micropharmacology of Monoclonal Antibodies in Solid Tumors : Direct Experimental Evidence for a Binding Site Barrier Micropharmacology of Monoclonal Antibodies in Solid Tumors : Direct Experimental Evidence for a Binding Site Barrier. Cancer Res. 1992; 52:5144-53.
12. Weinstein JN, van Osdol W. The macroscopic and microscopic pharmacology of monoclonal antibodies. Int J Immunopharmacol. 1992; 14:457-63.
13. Weinstein JN, van Osdol W. Early intervention in cancer using monoclonal antibodies and other biological ligands: micropharmacology and the "binding site barrier". Cancer Res. 1992; 52:2747-2751.
14. Juweid M, Neumann R, Paik C, Perez-Bacete MJ, Sato J, van Osdol W, et al. Micropharmacology of monoclonal antibodies in solid tumors: direct experimental evidence for a binding site barrier. Cancer Res. 1992; 52:5144-53.
15. Mitsunaga M, Ogawa M, Kosaka N, Rosenblum LT, Choyke PL, Kobayashi H. Cancer cell–selective in vivo near infrared photoimmunotherapy targeting specific membrane molecules. Nat Med. 2011; 17:1685-91.
16. Carcinoma I-RH, Kreitman BRJ, Bailon P, Chaudhary VK, Fitzgerald DJP, Pastan I. Recombinant immunotoxins containing anti-Tac(Fv) and derivatives of Pseudomonas exotoxin produce complete regression in mice of an interleukin-2 receptor-expressing human carcinoma. Blood. 1994; 83:426-34.
17. Tumors I-R, Webber KO, Kreitman RJ, Pastan I, Webber K. Rapid and Specific Uptake of Anti-Tac Disulfide-stabilized Fv by Rapid and Specific Uptake of Anti-Tac Disuffide-stabiized Fv by Interleukin-2 Receptor-bearing Tumors. Cancer Res. 1995; 55:318-23.
18. Barrett T, Koyama Y, Hama Y, Ravizzini G, Shin IS, Jang B-S, et al. In vivo diagnosis of epidermal growth factor receptor expression using molecular imaging with a cocktail of optically labeled monoclonal antibodies. Clin Cancer Res. 2007; 13:6639-48.
19. Mitsunaga M, Nakajima T, Sano K, Choyke PL, Kobayashi H. Near Infrared Theranostic Photoimmunotherapy (PIT): Repeated Exposure of Light Enhances the Effect of Immunoconjugate. Bioconjug Chem. 2012; 23:604-9.
20. Krupp MN, Connolly DT, Lane MD. Synthesis, turnover, and down-regulation of epidermal growth factor receptors in human A431

epidermoid carcinoma cells and skin fibroblasts. J Biol Chem. 1982; 257:11489-96.

21. Lopez JG, Chew J, Thompson HW, Malrer JS. EGF Cell Surface Receptor Quantitaiion on Ocular Cells by an Immunocytochemical Flow Cyfometry Technique. Invest Ophthalmol Vis Sci. 1992; 33:2053-62.

22. Yu JS, Chen HC, Yang SD. Reversible tyrosine phosphorylation/dephosphorylation of proline-directed protein kinase FA/glycogen synthase kinase-3alpha in A431 cells. J Cell Physiol. 1997; 171:95-103.

23. Koyama Y, Barrett T, Hama Y, Ravizzini G, Choyke PL, Kobayashi H. In vivo molecular imaging to diagnose and subtype tumors through receptor-targeted optically labeled monoclonal antibodies. Neoplasia. 2007; 9:1021-9.

24. Topp EM, Kitos PA, Vijaykumar V, DeSilva BS, Hendrickson TL. Antibody transport in cultured tumor cell layers. J Control Release. 1998; 53:15-23.

25. Fazio F, Paganelli G. Antibody-guided scintigraphy: targeting of the "magic bullet". Eur J Nucl Med. 1993; 20:1138-40.

26. Kimura H, Lee C, Hayashi K, et al. UV light killing efficacy of fluorescent protein-expressing cancer cells in vitro and in vivo. J Cell Biochem. 2010; 110:1439-46.

27. Tsai M, Aki R, Amoh Y, et al. GFP-fluorescence-guided UVC irradiation inhibits melanoma growth and angiogenesis in nude mice. Anticancer Res. 2010; 30:3291-4.

28. Momiyama M, Suetsugu A, Kimura H, et al. Fluorescent proteins enhance UVC PDT of cancer cells. Anticancer Res. 2012; 32:4327-30.

29. Momiyama M, Suetsugu A, Kimura H, et al. Imaging the efficacy of UVC irradiation on superficial brain tumors and metastasis in live mice at the subcellular level. J Cell Biochem. 2013; 114:428-34.